The melatonergic agonist agomelatine ameliorates high fat diet-induced obesity in mice through the modulation of the gut microbiome.

Patricia Diez-Echave[1], Teresa Vezza[2], Francesca Algieri[3], Antonio Jesus Ruiz-Malagon[1], Laura Hidalgo Garcia[3], Federico Garcia[4], Rocio Moron[5], Manuel Sanchez-Santos[6], Marta Toral [1], Miguel Romero[6], Juan Duarte[7], Jose Garrido-Mesa[1], Maria Elena Rodriguez-Cabezas[8], Alba Rodrguez-Nogales[9], and Julio Galvez[6]

[1]CIBER-EHD, Department of Pharmacology, Center for Biomedical Research (CIBM), University of Granada
[2]University of Granada
[3]CIBER-EHD, Department of Pharmacology, ibs.GRANADA, Center for Biomedical Research (CIBM), University of Granada, Granada, 18011
[4]Complejo Hospitalario Universitario de Granada
[5]Instituto de Investigacion Biosanitaria de Granada (ibs.GRANADA)
[6]University of Granada Faculty of Pharmacy
[7]University ofGranada
[8]CIBER-EHD, University of Granada
[9]1 CIBER-EHD, Department of Pharmacology, Center for Biomedical Research (CIBM), University of Granada

April 16, 2024

Abstract

Background and Purpose: Melatonin has shown bene cial e ects on obesity, both in humans and experimental models, via regulating the altered circadian rhythm and thus ameliorating the gut dysbiosis associated with this metabolic condition. However, its clinical use is limited, mostly due to its short half-life. Agomelatine is an agonist of the melatonin receptors that could be used to manage obesity and o er a better pro le than melatonin. Experimental Approach: Male C57BL/6 mice were fed a high fat diet and orally treated for ve weeks with agomelatine, or melatonin or metformin, used as control drugs. Metabolic pro le, in ammatory status, vascular dysfunction and intestinal microbiota composition were assessed. Key Results: Agomelatine lessened body weight gain, enhanced glucose and lipid metabolisms, and improved insulin resistance. It also reduced the obesity-associated in ammatory status and endothelial dysfunction, probably linked to its e ect on gut dysbiosis, consisting of the restoration of bacterial populations with key functions, such as short chain fatty acid production. Conclusions and Implications: Agomelatine can be considered as a novel therapeutic tool for the management of human obesity and its associated comorbidities.

1. Introduction

Obesity is highly prevalent, with 1.9 billion overweighted adults, being 650 million obese. It represents a major worldwide public health challenge that reduces life expectancy by 0.9 to 4.2 years and causes the death of 3.4 million adults per year (WHO, 2019).

Obesity is typically associated with `poor' diets, high in fat and low in dietary bre. Mechanistically, this is related to insulin resistance, resulting in dysregulation of glucose and lipid metabolisms, together with development of low-grade systemic in ammation. In ltration of activated immune cells in metabolic tissues, including liver and fat, leads to proin ammatory cytokine secretion and re-programming of immunoregulatory cells. These alterations raise the risk of comorbidities, like metabolic syndrome, non-alcoholic fatty liver disease (NAFLD), type 2 diabetes and/or cardiovascular diseases(Targher, Byrne, Lonardo, Zoppini, & Barbui, 2016).

The gut microbiome is also involved in the pathogenesis of obesity. Development of obesity and the associated in ammation and insulin resistance have been related to dysbiosis, modi cations in the composition and/or function of the intestinal microbiota. This has also been linked to the impairment of energy homeostasis and gut permeability(Shen et al., 2013). Therefore, alleviating gut dysbiosis in experimental models has shown to e ectively prevent and treat obesity and its related disorders(Muscogiuri et al., 2019).

In addition, the circadian rhythm and the lipid metabolism are nowadays accepted to cross-regulate through di erent mechanisms that include hormones like melatonin, leptin or glucocorticoids, intestinal microbiome and energy metabolism. Its dysregulation may be also associated with the risk of obesity, which may subsequently worsen circadian clocks(Li et al., 2020).

In this regard, melatonin, which is an important regulator of the circadian rhythm(Reiter, Tamura, Tan, & Xu, 2014), oxidative stress(Zhang & Zhang, 2014), immune function(Liu et al., 2017), and glucose and lipid metabolism(Cipolla-Neto, Amaral, Afeche, Tan, & Reiter, 2014), has been described to also prevent obesity in high fat diet-fed mice, thus leading to gut microbiota modulation, by restoring Firmicutes / Bacteroidetes ratio and raisingAkkermansia abundance(Abuqwider, Mauriello, & Altamimi, 2021). Moreover, melatonin has been reported to improve lipid metabolism and reduce hepatic lipid accumulation and steatosis, maybe through gut microbiota reprogramming, as well(Yin et al., 2018). However, melatonin displays an extremely short half-life (under 30 min), which hinders its clinical application, but it provides new insights for the melatoninergic pathway-based therapeutics. Hence, di erent melatonin agonists, with better pharmacokinetics and longer half-times, have been developed. Among these, agomelatine is an agonist of the melatonin receptors MT1 and MT2, but also an antagonist of 5-HT2B and 5-HT2C serotonin receptors(Hickie & Rogers, 2011). Agomelatine shows potent antidepressant and anxiolytic properties and is licensed for the management of major depressive disorders in adults(Gorwood et al., 2020). Recently, it has been reported its anxiolytic/antidepressant e ect in obese rats, maybe due to an amelioration of the high fat diet (HFD)-associated in ammation and oxidative stress(Rebai, Jasmin, & Boudah, 2021). Therefore, a comprehensive study of the e ects of agomelatine would be necessary to consider its therapeutic value in these conditions. With this aim, agomelatine was assayed in an experimental model of obesity induced by a HFD in mice. Its e ect was compared to that of melatonin and metformin, which has been used as a weight loss drug(Pu et al., 2020) and their impact on metabolic pro le, in ammatory response, vascular dysfunction and gut microbiota composition was evaluated.

2. Materials and Methods

2.1. Materials

All the chemicals were purchased from Sigma-Aldrich Quimica SL (Madrid, Spain), unless otherwise speci ed.

2.2. Animals and experimental design.

The study was performed in agreement with the `Guide of the Care and Use of Laboratory animals' as promulgated by the National Institute of Health and all procedures were approved by the Ethics Committee of Laboratory Animal of the University of Granada (Spain) (Ref. No. 28/03/2016/030). Eight-week-old male C57BL/6 mice obtained from Janvier labs (St. Berthevin, Cedex, France) were housed in makrolon cages, maintained under controlled light-dark cycle (12 h light/dark cycle), temperature and relative humidity (22 ± 1ºC, 55 ± 10%) and provided with a free access to tap water. Mice were fed with either a standard chow diet (13% calories from fat, 20% calories from protein and 67 % calories from carbohydrate; Global

diet 2014; Harlan Laboratories, Barcelona, Spain) or a high fat diet (HFD) (59% calories from fat, 13% calories from protein and 28% calories from carbohydrate; Puri ed diet 230 HF; Scienti c Animal Food & Engineering, Augy, France). They were randomly divided in seven groups (n=8): control diet, HFD and ve HFD-treated groups. Mice were daily treated by oral gavage with melatonin (15mg/kg), agomelatine (10, 25 and 50 mg/kg) or metformin (250 mg/kg) dissolved in water for ve weeks (more detail in supplementary). Animal body weight and food and water intake were regularly controlled, and feed e ciency was calculated as the ratio of body weight gain (g) to caloric intake (kcal). One week before the sacri ce, a glucose tolerance test was performed. At the end of the experiment, mice were fasted overnight, a blood sample was collected by cardiac puncture under iso urane anaesthesia and then sacri ced by cervical dislocation (Figure 1).

2.3. Glucose tolerance test

At week 4, mice fasted for 8 h were given a 50% glucose solution in water (2 g/kg of body weight) by intraperitoneal injection, and a blood sample was taken from the tail vein before glucose administration and 15, 30, 60 and 120 min after. Blood glucose was determined with a handheld glucometer (Contour XT, Ascensia Diabetes Care, S.L., Barcelona, Spain).

2.4. Plasma Determinations

Blood samples were taken on the day of sacri ce in heparin blood collection tubes and centrifuged for 20 min at 5000g at 4°C. The plasma was frozen at -80°C until further analysis. Plasma glucose, LDL (low-density lipoprotein)-cholesterol and HDL (high-density lipoprotein)-cholesterol concentrations were measured by colorimetric methods using Spinreact kits (Spinreact, S.A., Girona, Spain). Plasma insulin levels were quan-ti ed using a mouse insulin ELISA kit (Alpco Diagnosis, Salem, NH, USA). Homeostatic model assessment of insulin resistance (HOMA-IR) was computed with the formula: fasting glucose (mM) Ö fasting insulin (mU/mL) / 22.5.

2.5. Morphological variables

After sacri ce, liver and abdominal and epididymal fat were collected, cleaned, and weighed. Fat/weight index was estimated by dividing body weight by tibia length. The samples were then frozen in liquid nitrogen and stored at -80°C.

2.6. Vascular reactivity studies and NADPH oxidase activity

Descending thoracic aortic rings were dissected to assess obesity-associated vascular dysfunction by measuring acetylcholine vasorelaxant ability and NADPH oxidase activity.

For the vascular reactivity study, the organ chamber was lled with Krebs solution (composition in mM: NaCl 118, KCl 4.75, $NaHCO_3$ 25, $MgSO_4$ 1.2, $CaCl_2$ 2, KH_2PO_4 1.2 and glucose 11) at 37 degC and gassed with 95% O_2 and 5% CO_2 (pH 7.4). Length-tension characteristics were obtained via the myograph software (Myodaq 2.01 (Danish Myotechnologies, Denmark)) and the aortae were loaded to a tension of 5 mN. After the stabilization period, cumulative concentration-response curves to acetylcholine (10^{-9} M-10^{-5} M) were performed in intact rings pre-contracted by U46619 (10^{-8} M). Relaxant responses to acetylcholine were expressed as a percentage of pre-contraction.

The evaluation of NADPH oxidase activity in aortic rings was performed by lucigenin-enhanced chemilu-minescence assay. Aortic rings were incubated for 30 min at 37 degC in HEPES-containing physiological salt solution (pH 7.4; in mM: NaCl 119, HEPES 20, KCl 4.6, $MgSO_4$ 1, Na_2HPO_4 0.15, KH_2PO_4 0.4, $NaHCO_3$ 1, $CaCl_2$ 1.2 and glucose 5.5). To stimulate the aortic production of O^{2-}, the rings were incubated with NADPH (100 mM). Consequently, the aortic rings were then placed in tubes containing physiological salt solution, with or without NADPH and lucigenin was injected automatically at a nal concentration of 5 mmol/L. NADPH oxidase activity were determined by measuring luminescence over 200 s in a scintillation counter (Lumat LB 9507, Berthold, Germany) in 5-s intervals and was calculated by subtracting the basal values from those in the presence of NADPH. Vessels were then dried, and dry weight was determined. NADPH oxidase activity is expressed as relative luminescence units (RLU)/min/mg dry aortic ring.

2.7. Analysis of gene expression by RT-qPCR

Total RNA was extracted from liver and fat samples using TRIzol® Reagent (Invitrogen Life Technologies, Carlsbad, CA, USA), following the manufacturer's recommendations, and was reverse transcribed into cDNA using oligo(dT) primers (Promega, Southampton, UK). Real time quantitative PCR (qPCR) ampli cation and detection was carried out on optical-grade 48 well plates in EcoTM Real time PCR System (Illumina, San Diego, CA, USA) with 20 ng of cDNA, the KAPA SYBR (r) FAST qPCR Master Mix (Kapa Biosystems, Wilmington, MA, USA) with speci c primers (Table 1). The mRNA relative quantitation was calculated using the DD Ct method and glyceraldehyde 3-phosphate dehydrogenase (Gapdh) was used as housekeeping gene.

2.8. Flow cytometry

The cells from adipose and liver tissues were collected following the procedure previously described with some modi cations(Anderson, Carrillo-Galvez, & Martn, 2015). $CD45^+CD11b^+$ and $CD11b^+Ly6C^+$

2.9. DNA extraction and Illumina MiSeq sequencing

Faecal DNA was isolated as described(Rodriguez-Nogales et al., 2017). The resultant sequences were quality- ltered, clustered, and taxonomically allocated against the SILVA database with 97% similarity threshold using the QIIME software package (Version 1.9.1) (Knight Lab, San Diego, CA, USA). The resulting abundance was used to compute the total bacterial diversity in an equivalent manner.

DNA from fecal contents was isolated following the procedure described by Rodrguez-Nogales et al. 2017(Rodriguez-Nogales et al., 2017). Total DNA from faecal samples was PCR ampli ed using primers targeting regions anking the variable regions 4 to 5 of the bacterial 16S rRNA gene (V4-5), gel puri ed, and analyzed using multiplexing on the Illumina MiSeq machine. PCR reactions from the same samples were cleaned and then normalized using the high-throughput Invitrogen SequalPrep 96-well Plate kit. Later, a library from the samples was made uorometrically to be quanti ed uorometrically before sequencing.

The resulting sequences were completed, quality- ltered, clustered, and taxonomically assigned on the basis of 97% similarity level against the RDP (Ribosomal Database Project) by the QIIME software package (Version 1.9.1) (Knight Lab, San Diego, CA, USA). Sequences were selected to estimate the total bacterial diversity of the DNA samples in a comparable manner and were trimmed to remove barcodes, primers, chimeras, plasmids, mitochondrial DNA and any non-16S bacterial reads and sequences <150 bp.

Alpha diversity (a-diversity) indices and bacterial abundance data were compared using Kruskal{Wallis test followed by pairwise Mann{Whitney U comparison. Resulting p-values were corrected by the Bonferroni method. Analysis of a-diversity was performed on the output normalized data, which were evaluated using Mothur. The biomarkers for both species taxonomic analysis and functional pathways via calculation of the linear discriminant analysis (LDA) score among di erent phenotype groups were calculated by LEfSe (linear discriminatory analysis (LDA) e ect size) (Version 1.0). Principal coordinate analysis (PCoA) was performed to identify principal coordinates and visualize b-diversity in complex multidimensional data of bacteriomes from di erent groups of mice. Di erences in b-diversity were tested by permutational multivariate analysis of variance (PERMANOVA) using the web-based algorithm tool Microbiome Analyst (Dhariwal et al., 2017). The data are expressed as the mean ± standard error of the mean (SEM). Experimental data were analysed in GraphPad Prism 8 (GraphPad Software, Inc., La Jolla, CA, USA) by one-way or two-way ANOVA or Pearson correlation. Data with $p < 0.05$ were considered statistically signi cant. Metabolic phenotypes were obtained by genera classi cation according to their primary fermentation products as acetate, butyrate, lactate, or other producers using Bergey's Manual of Systematic Bacteriology(Boone, Castenholz, & Garrity, 2001). The genera with unknown or ambiguous fermentative products were excluded. Major genera were classi ed according to the dominant fermentation end-product(s).

Hierarchical clustering and heat maps depicting the metabolic parameters, patterns of abundance and log values were constructed within the \R" statistical software package (version 3.6.0; https://www.r-project.org/) using the "pheatmap", \heatmap.2" and \ggplots" packages. Spearman's correlations of bacterial taxa with

metabolic parameters and KEGG metagenomic functions were calculated in \R". Co-occurrence networks between taxa and functions were calculated by using the open-source software Gephi (https://gephi.org/) to nd di erential associations caused by similar alterations in the proportion of di erent taxa and their predicted functions between di erent groups of mice. Modularity-based co-occurrence networks were analysed at a Spearman's correlation cut o 0.7 and $p < 0.01$; the selected correlation data were imported into the interactive platform, Gephi (version 0.9.2; https://gephi.org), and the following modularity analyses and keystone node identi cation were conducted within Gephi.

2.10. Statistics

All results are expressed as the mean ± SEM. Di erences between means were assessed for statistical signi cance with a one-way analysis of variance (ANOVA) and post-hoc least signi cance tests. Di erences between proportions were examined with the chi-squared test. All statistical analyses were performed with the GraphPad 8 software package (GraphPad Software, Inc., La Jolla, CA, USA), with statistical signi cance set at $p < 0.05$.

3. Results

3.1. Agomelatine reduces body weight and ameliorates the altered plasma biochemical pro le in HFD-fed mice.

The administration of agomelatine (10, 25 and 50 mg/kg) to HFD-fed mice signi cantly lessened body weight gain compared to untreated control obese mice (Figure 2A). Agomelatine did not present an anorexigenic e ect since it did not modify the total energy intake but lowered the energy e ciency (Figure 2B) and consequently reduced epididymal and abdominal fat deposits (Figure 2C). Similar e ects were seen in obese mice treated with melatonin (15 mg/kg) or metformin (250 mg/kg) (Figure 2A-C).

Mice receiving agomelatine also showed lower plasma glucose concentrations at all time points compared to untreated HFD-fed control mice (Figure 3A), thus resulting in signi cant reductions in the area under the curve (AUC) (Figure 3A). Accordingly, these mice displayed signi cantly reduced values of the HOMA-IR index (Figure 3B), a marker of insulin intolerance calculated with the fasting insulin (Figure 3B) and glucose values (Figure 3B) nsout. In fact, the mice treated with 50 mg/kg of agomelatine showed similar HOMA-IR index to control mice. Likewise, melatonin and metformin ameliorated the glucose intolerance status (Figure 3B).

Regarding the lipid pro le, the untreated HFD-fed group presented a hypercholesterolemic status, with higher levels of total cholesterol, LDL- and HDL-cholesterol than control diet fed mice. As expected, metformin treatment signi cantly ameliorated the alterations in the cholesterol pro le, reducing total and LDL-cholesterol (Figure 3C). Interestingly, agomelatine treatment signi cantly improved the cholesterol pro le in the same way as metformin, whereas melatonin had no e ect on LDL-cholesterol and only signi cantly reduced HDL-cholesterol (Figure 3C).

3.2. Agomelatine treatment improves the in ammatory status in obese mice.

Non-treated HFD mice displayed an ampli ed expression of Tnf-a , Il-1b , Il-6 and monocyte chemotactic protein 1 (Mcp-1) in adipose tissue (Figure 4A) and liver (Figure 4A), compared to control mice. All the treatments reduced the expression of those pro-in ammatory mediators in the liver, but only agomelatine reduced their expression in fat tissue (Figure 4A). Likewise, the expression of Jnk-1 was signi cantly up-regulated in the liver of untreated obese mice in comparison with non-obese ones, which was also signi cantly lowered by all treatments (Figure 4B).

Elevated fat expression of leptin in the HFD group (Figure 4C) was linked to a decreased expression of leptin receptors in liver and fat (Figure 4C). Regarding adiponectin, obese mice presented a lower expression in adipose tissue nsout. However, agomelatine and metformin were able to signi cantly increase them (Figure 4C).

Expression of Glut-4 in fat of HFD-fed mice was decreased in comparison with non-obese mice (Figure 4D). Melatonin treatment did not show any effect but agomelatine (50 mg/kg) and metformin were able to increase its expression (Figure 4D).

Non-treated HFD-fed mice displayed a reduced expression of Ampk while agomelatine and metformin treatments reverted it, both in liver and fat (Figure 4D).

The flow cytometry analysis showed that the total number of MDSCs ($Ly6C^+$ $CD11b^+$) cells in liver was increased in obese mice compared to control mice although all treatments restored their accumulation in liver (Figure 5). Regarding the macrophages, obese mice showed a significant infiltration of $CD45^+CD11b^{int}$ cells in liver and fat tissue. However, in the treated mice, no significant differences were observed in comparison with the lean ones. Moreover, agomelatine, at all doses, significantly reduced the number of this cell type in the liver, normalizing it, and at the highest dose the fat tissue (Figure 5).

3.3. Agomelatine treatment ameliorates intestinal barrier dysfunction.

Mucosal integrity appeared compromised in untreated HFD-fed mice, demonstrated by a down-regulation of intestinal epithelial markers, such as Muc-2 , Muc-3 , Occludin , T -3 and Zo-1 (Figure 6A). The administration of agomelatine and melatonin was able to increase the expression of these markers (Figure 6A). Obese mice also displayed a higher expression of Tlr-4 in liver (Figure 6B) which was downregulated by all the treatments.

3.4. Agomelatine treatment restores the gut dysbiosis in obese mice.

This study explores for the first time the effect of agomelatine on gut microbiota. Only the highest dose (50mg/kg) was evaluated since it was the one that showed a greater effect in the macroscopic and biochemical parameters.

Several ecological features were determined, including Chao1 richness (diversity estimation), Observed OTUs (count of unique OTUs in each sample) and Shannon diversity (a richness and evenness estimator). Microbial richness, evenness and diversity were significantly decreased in the HFD group compared to non-obese mice. Although all treatments were able to increase these ecological parameters, only agomelatine significantly restored all of them (Figure 7). The principal coordinates analysis (PCoA) showed evident differences between control diet- and HFD-fed groups, indicative of extremely different gut environments (Figure 7B). Interestingly, the treatments displayed marked shifts in the obese gut microbiome (Figure 7B). Further analysis at phylum level (Figure 7C) revealed that HFD induced a dramatic change in the two most abundant phyla when compared to non-obese mice, significantly increasing Firmicutes and reducing Bacteroidetes (Figure 7C). Agomelatine significantly restored to baseline F/B ratio (Figure 7C). Verrucomicrobia phylum was also reduced in the HFD-fed group but agomelatine restored it (Figure 7C).

At order level, untreated HFD mice presented a reduced proportion in the sequences of Bacteroidales, Verrucomicrobiales and Lactobacillus whilst Erysipelotrichales ,Clostridiales and Lachnospirales abundance were significantly increased (Figure 8). Agomelatine treatment showed a similar profile than non-obese mice while metformin only counteracted some of the altered orders (Figure 8). When the functional-gene profile was assessed, our results showed a clear difference between non-obese mice and un-treated HFD ones (Figure 9A). Interestingly, the treatments also produced an important change in this profile, which was more accentuated in the case of agomelatine and metformin (Figure 9A). Thus, while metformin increased the bacterial genes associated with tryptophan, fructose and mannose metabolism and with glycosaminoglycan degradation, agomelatine up-regulated the genes involved in glycolysis, gluconeogenesis and lipid metabolism (Figure 9A), and decreased genes involved in the transport (including ABC transporter), bacterial secretion, PPAR signalling, fatty acid biosynthesis, motility and sugars assimilation, along with others, which appeared increased in HFD-mice (Figure 9A).

Agomelatine also had a clear effect on short chain fatty acids (SCFA)-producing bacteria. Non-treated HFD-fed mice showed a decrease in butyrate-producing bacteria abundance in comparison with non-obese mice (Figure 9B), but oral administration of agomelatine and metformin significantly increased the relative

abundance of butyrate-producing bacteria (Figure 9B). Propionate-producing bacteria were also reduced by HFD intake (Figure 9B) although all treatments increased the abundance of these bacteria, being agomelatine the most relevant (Figure 9B). Interestingly, agomelatine also augmented the abundance of A. muciniphila (Figure 9C), a propionate producing bacteria(Louis & Flint, 2017).

3.5. Agomelatine supplementation enhances endothelial function

The endothelium-dependent vasodilator response to acetylcholine of aortic rings was measured to analyse the functionality of the endothelium. The results showed a reduction in vasodilatory responses in the HFD group in comparison with control mice (Figure 10A). Improved endothelial relaxation could be observed in mice treated with the highest doses of agomelatine, as well as with melatonin and metformin. Since this could be related to the oxidative stress, the activity of the enzyme NADPH, the main source of reactive oxygen species in this location, was measured. Obese mice exhibited a more pronounced activation than the lean ones. The highest doses of agomelatine, melatonin and metformin downregulated it (Figure 10B).

4. Discussion

Dysregulation of circadian rhythm homeostasis has been associated with various disorders of lipid metabolism, including obesity(Li et al., 2020). In this sense, melatonin has been explored as a treatment for obesity and other metabolic disorders. Since con icting results have been reported(Genario, Cipolla-Neto, Bueno, & Santos, 2021; Loloei et al., 2019), a more in-depth investigation is required to develop innovative therapeutic strategies. With this aim, we evaluated the e ect of agomelatine, a melatonergic agonist, in experimental obesity in mice, and compared it to melatonin and metformin, the most prescribed antidiabetic drug.

Our results show that agomelatine treatment lowered body weight gain and fat accumulation in a similar manner to previously observed for melatonin(de Farias et al., 2019) and metformin(Ji, Wang, & Li, 2019), as well as improved obesity-associated glucose intolerance. This con rms previous experimental observations that associate weight decrease and enhanced insulin sensitivity with the regulation of metabolic clock and/or the increase of the energy expenditure/intake ratio(Cherngwelling et al., 2021; Farias et al., 2019). Although some preclinical studies have indicated that melatonin lowers body weight and visceral fat accumulation(de Farias et al., 2019; Farias et al., 2019), this has not been con rmed in humans(Mantele et al., 2012). However, it has been observed that agomelatine administration in patients with night eating syndrome reduces body weight, related to restoration of sleep patterns and sleep-related eating disorders(Milano et al., 2013), and its anti-obesogenic has been recently reported in HFD-fed rats(Cherngwelling et al., 2021), in agreement with our observations.

Regarding the lipid pro le, whereas melatonin only reduced HDL-cholesterol, agomelatine supplementation showed a signi cant improvement in the cholesterol pro le. This e ect could be related to the direct e ect of the circadian rhythms regulating dietary lipid absorption in intestinal enterocytes(Hussain & Pan, 2012). Metformin treatment also ameliorated the hypercholesterolemic status induced by HFD, an e ect widely described in humans and mice(Gonzalez & Jiang, 2017), lightening the severity of high fat induced hepatic steatosis.

The accumulation of fat tissue in obesity is linked to a chronic low-grade in ammation, with elevated circulating proin ammatory mediators, such as TNF- a and IL-6 secreted by the liver and fat tissue(Ellulu, Patimah, Khaza'ai, Rahmat, & Abed, 2017). This drives immune cell recruitment and activation of in ammatory signalling pathways, such as the c-Jun N-terminal kinase (JNK)-related signalling, which interferes with insulin signalling, and therefore, with the glucose metabolism(Lee, Giraud, Davis, & White, 2003). Consistently, HFD led to augmented expression of di erent pro-in ammatory mediators, including Tnf-a , Il-1b ,Il-6 and Mcp-1 , in adipose tissue and liver. While all the treatments reduced their expression in the liver, only agomelatine reduced them in fat tissue. Likewise, all treatments signi cantly lowered HFD-induced Jnk-1 up-regulation, in line with previous results(Farias et al., 2019). Nevertheless, this is the rst report of such anti-in ammatory activity for agomelatine treatment in obese mice, which could participate in the improvement of insulin signalling and glucose metabolism.

The excessive accumulation of adipose tissue can also produce an alteration in adipokine levels, such as leptin and adiponectin. Leptin, apart from suppressing appetite, is considered a pro-in ammatory mediator associated with insulin resistance(Yadav et al., 2013). In obesity, decreased expression of the leptin receptor in liver and fat lead to leptin resistance and excessive leptin release(Yadav et al., 2013). Conversely, adiponectin is an anti-in ammatory and insulin-sensitizing mediator that suppresses hepatic glucose production(Sharma, McClung, & Abraham, 2016). Altered leptin and adiponectin expression pro les were observed in this study. Lower fat expression of adiponectin in obese mice, which agrees with previous studies(Wu et al., 2021), was only signi cantly upregulated by agomelatine and metformin. Whilst metformin and melatonin have been widely assessed for their impact on adipokine production in experimental and human studies of obesity or diabetes(Ferreira-Hermosillo et al., 2020; Su et al., 2016), this is the rst evidence of bene cial impact of agomelatine on adiponectin and leptin expression.

Besides, obesity-related insulin resistance implies intracellular glucose uptake impairment due to reduced GLUT-4 expression. Such e ect was observed in HFD-fed mice and counteracted by agomelatine and metformin, but not melatonin, which neither has previously shown a signi cant e ect on pinealectomized animals(Nogueira et al., 2011). Also related with insulin resistance in obesity is the role of AMPK, involved in the translocation of GLUT-4 transporters to the membrane and the inhibition of liver gluconeogenesis and in ammatory pathways(Ruderman, Carling, Prentki, & Cacicedo, 2013). Antidiabetic drugs, including metformin, act as insulin sensitizers through AMPK activation(Lu et al., 2019). Hence,Ampk expression in liver and fat was partially restored by metformin, but also agomelatine. These results, together with the decreased glycaemia, con rm the capacity of the agomelatine treatment to improve insulin sensitivity and glucose homeostasis facilitated by central and peripheral target tissues. In addition to energy metabolism, AMPK is also recognized as a regulatory node for immune responses(O'Neill & Hardie, 2013). AMPK activation inhibits two major immune signalling pathways, nuclear factor- kB (NF- kB) and signal transducer and activator of transcription (STAT), reducing proin ammatory cytokines expression(Salminen, Hyttinen, & Kaarniranta, 2011). This anti-in ammatory e ect was also evidenced mainly in agomelatine-treated mice, reducing cytokine expression and immune cell in ltration.

Under pathological conditions, like obesity, the pro-in ammatory milieu stimulates the proliferation immature myeloid cells (IMCs) and block the di erentiation into mature myeloid populations, causing the accumulation of myeloid-derived suppressor cells (MDSCs) ($Ly6C^{+}CD11b^{+}$). The liver is the major organ where IMCs accumulate(Budhwar, Verma, Verma, Rai, & Singh, 2018), and, in agreement with previous studies(Sundara Rajan & Longhi, 2016), we observed an increase of MDSCs in obese mice. HFD could lead to immune activation and recruitment, as shown above by increased IL-6 liver expression, and reported for NAFLD patients, explaining the impaired myeloid di erentiation(Braunersreuther, Viviani, Mach, & Montecucco, 2012). Interestingly, all treatments restored its accumulation as well as IL-6 expression levels in this experimental model, which has also previously been observed for metformin *in vivo* (Hayashi et al., 2019) and *in vitro* (Xu et al., 2019).

Macrophages are key regulators of the in ammatory process, reacting to a wide variety of stimuli, including metabolic signals. It is well known that the accumulation of in ammatory macrophages in the liver and in the fat contributes to the deregulation of glucose homeostasis, obesity-induced in ammation, and hepatic brosis. The hepatic macrophage population ($CD45^{+}CD11b^{int}$) was increased in obese mice and, both melatonin and metformin reduced it, as expected from other studies(de Farias et al., 2019; Woo et al., 2014). Interestingly, agomelatine showed an even stronger e ect at the highest dose, and it also restored macrophage population in the adipose tissue, con rming the improvement of the in ammatory response in association with the metabolic status.

Obesity has also been associated with an increased gut permeability, which positively correlates with HOMA-IR index and is aggravated by liver injury(Teixeira, Souza, et al., 2012). In line with the loss of mucosal integrity, we observed a down-regulation of intestinal epithelial markers in obese mice, which could enable the access of bacterial components, such as LPS, into the circulation, contributing to the underlaying in ammation(Luther et al., 2015). Agomelatine and melatonin increased the expression of these markers and,

as a consequence, counteracted the upregulation of liver TLR-4 expression, which correlates with LPS plasma levels(Diez-Echave et al., 2020). This impact in TLR4, which promotes NF-kB signalling and the subsequent release of cytokines, adipokines and ROS, could also explain the bene cial e ect of agomelatine, connecting intestinal permeability with improved in ammatory response and glucose and lipid homeostasis.

Regarding microbiota composition, as commented before, obesity-associated dysbiosis may contribute to metabolic endotoxemia and thus low-grade systemic in ammation. Interestingly, it has been previously shown that melatonin and metformin treatments can also reverse gut dysbiosis associated with metabolic endotoxemia in animal models of obesity(Ren et al., 2018; Zhang & Hu, 2020). Thus, we studied microbial composition and observed a decrease in microbial richness, evenness and diversity associated with HFD intake. Agomelatine has shown for the rst time to produce marked shifts in the obese gut microbiome and restore the balance between Firmicutes and Bacteroidetes, of interest for the management of the metabolic syndrome and obesity(Shen et al., 2013). The increase in Firmicutes / Bacteroidetes (F/B) ratio has been associated with a more e cient hydrolysis of non-digestible polysaccharides and an increased caloric use in obese individuals(Shen et al., 2013). Other alterations described in obese patients, such as reduced Verrucomicrobia phylum(Crovesy, Masterson, & Rosado, 2020), were also observed in our model and restored by agomelatine treatment. At lower taxonomic levels, agomelatine also normalized the composition of microbiota whilst metformin only had a partial e ect. It is particularly interesting the increase in Verrumicrobiales containing Akkermansia muciniphila , a mucin-degrading bacterium whose abundance is inversely associated with body weight in obese mice and type 2 diabetes(Abuqwider, Mauriello, & Altamimi, 2021). Treatments that stimulate its growth have shown to alleviate HFD-induced metabolic disorders(Abuqwider, Mauriello, & Altamimi, 2021), which points this as an interesting mechanism that could underlie agomelatine's bene cial e ects.

The "dialogue" between the intestinal microbiota and the host primarily relies on their biochemical pathways and metabolites produced, nding an altered functional pro le with HFD, which was evidenced in our study. Imputed gene expression and pathway analysis showed that agomelatine treatment correlates with an increase in glycolysis, gluconeogenesis and lipid metabolism, and underrepresentation of genes involved in the transport (including ABC transporter), bacterial secretion, PPAR signalling, fatty acid biosynthesis, motility and sugars assimilation(Greenblum, Turnbaugh, & Borenstein, 2012).Of note, agomelatine, together with metformin, increased the abundance of butyrate-producing bacteria, which have been describe to protects animals from HFD-induced obesity, attenuating fat gain and insulin resistance(Henagan et al., 2015). These results could be associated with the modi cation of the Bacteroidetes and Lactobacillus abundance, which participate in butyrate generation via lactate production(Le Chatelier et al., 2013), whilst the increase in propionate-producing bacteria could relate to A. muciniphila, a propionate producer bacteria(Louis & Flint, 2017). Moreover, propionate plays a key role in counteracting cholesterol synthesis, being the ratio acetate/propionate crucial for cholesterol and lipid metabolism regulation(Wong, de Souza, Kendall, Emam, & Jenkins, 2006). These results support the bene cial e ect observed with agomelatine and highlight its therapeutic potential for the modulation of the gut microbiota in obesity.

All the alterations observed in obesity, and in this experimental model, such as insulin signalling impairment, intestinal dysbiosis and systemic in ammation, can a ect endothelial function. An increased NADPH enzyme activity and the subsequent production of reactive oxygen species inactivates NO and impair vessel dilation, which contributes to the pathogenesis of the metabolic syndrome(Rovella et al., 2021). The decreased enzyme activity observed with agomelatine treatment could explain the enhanced endothelial relaxation, as well as the general improvement of the underlying condition.

In conclusion, the melatonergic agonist agomelatine improves glucose intolerance, insulin resistance, lipid metabolism and in ammatory status associated with HFD-induced obesity. Moreover, it has shown the ability to ameliorate the gut dysbiosis that characterizes this condition. These properties may support the use of agomelatine as a novel therapeutic tool to manage human obesity, which displays a better pharmacokinetic pro le than melatonin and more global e ects than this and metformin, the most used drug nowadays.

Acknowledgements

This work was supported by the Junta de Andaluca (CTS 164) and by Instituto de Salud Carlos III (PI19/01058) with funds from the European Union. T. Vezza is a postdoctoral fellow from Instituto de Investigacon Biosanitaria de Granada; P. Diez-Echave, F. Algieri and J. Garrido-Mesa are postdoctoral fellows from University of Granada; A.J. Ruiz-Malagon and L. Hidalgo-Garca are predoctoral fellows from University of Granada (\Programa de Doctorado: Medicina Clnica y Salud Rublica"). CIBER-EHD, CIBERCV and \Red de Investigacon en SIDA" are supported by Instituto de Salud Carlos III.

Author contributions

Patricia Diez-Echave, Teresa Vezza, Francesca Algieri, Antonio Jesus Ruiz-Malagon, Laura Hidalgo-Garca, Rocio Moron and Jose Garrido-Mesa performed the experiments and contributed to the acquisition and analysis of data. Marta Toral, Miguel Romero, Manuel Sanchez and Juan Duarte performed the vascular reactivity studies and NADPH oxidase activity experiment as well as their analysis. Alba Rodrguez-Nogales, Mara Elena Rodrguez-Cabezas, Julio Galvez and Federico Garcia contributed to the analysis and interpretation of data of microbiome analysis. Mara Elena Rodrguez-Cabezas, Julio Galvez, Jose Garrido-Mesa and Alba Rodrguez-Nogales designed the project and wrote the manuscript. All authors contributed to the revision.

Con ict of interest statement

The authors state no con ict of interests.

Data Availability Statement

Data available on request from the authors.

References

Abuqwider, J. N., Mauriello, G., & Altamimi, M. (2021). Akkermansia muciniphila, a New Generation of Bene cial Microbiota in Modulating Obesity: A Systematic Review. Microorganisms, 9 (5). doi: 10.3390/microorganisms9051098

Anderson, Per, Carrillo-Galvez, Ana Belen, & Martn, Francisco. (2015). Isolation of Murine Adipose Tissue-derived Mesenchymal Stromal Cells (mASCs) and the Analysis of Their Proliferation in vitro. Bio-protocol, 5 (21), e1642. doi: 10.21769/BioProtoc.1642

Boone, D.R., Castenholz, R., & Garrity, G. . (2001). Bergey's Manual of Systematic Bacteriology.Springer{ Verlag .

Braunersreuther, V., Viviani, G. L., Mach, F., & Montecucco, F. (2012). Role of cytokines and chemokines in non-alcoholic fatty liver disease. World J Gastroenterol, 18 (8), 727-735. doi: 10.3748/wjg.v18.i8.727

Budhwar, S., Verma, P., Verma, R., Rai, S., & Singh, K. (2018). The Yin and Yang of Myeloid Derived Suppressor Cells. Front Immunol, 9 , 2776. doi: 10.3389/ mmu.2018.02776

Cipolla-Neto, J., Amaral, F. G., Afeche, S. C., Tan, D. X., & Reiter, R. J. (2014). Melatonin, energy metabolism, and obesity: a review. J Pineal Res, 56 (4), 371-381. doi: 10.1111/jpi.12137

Crovesy, L., Masterson, D., & Rosado, E. L. (2020). Pro le of the gut microbiota of adults with obesity: a systematic review. Eur J Clin Nutr, 74 (9), 1251-1262. doi: 10.1038/s41430-020-0607-6

Cherngwelling, R., Pengrattanachot, N., Swe, M. T., Thongnak, L., Promsan, S., Phengpol, N., et al . (2021). Agomelatine protects against obesity-induced renal injury by inhibiting endoplasmic reticulum stress/apoptosis pathway in rats. Toxicol Appl Pharmacol, 425 , 115601. doi: 10.1016/j.taap.2021.115601

de Farias, Tdsm, Cruz, M. M., de Sa, Rcdc, Severi, I., Perugini, J., Senzacqua, M, et al . (2019). Melatonin Supplementation Decreases Hypertrophic Obesity and In ammation Induced by High-Fat Diet in Mice. Front Endocrinol (Lausanne), 10 , 750. doi: 10.3389/fendo.2019.00750

Farias, T., Paixao R.I.D., Cruz M.M., de Sa R., Simao, J.J., Antraco, V.J., Alonso-Vale, M.I.C. Melatonin Supplementation Attenuates the Pro-In ammatory Adipokines Expression in Visceral Fat from Obese Mice Induced by A High-Fat Diet, Cells 8(9) (2019).

Dhariwal, A., Chong, J., Habib, S., King, I. L., Agellon, L. B., & Xia, J. (2017). MicrobiomeAnalyst: a web-based tool for comprehensive statistical, visual and meta-analysis of microbiome data.Nucleic Acids Res, 45 (W1), W180-W188. doi: 10.1093/nar/gkx295

Diez-Echave, P., Vezza, T., Rodriguez-Nogales, A., Ruiz-Malagon, A. J., Hidalgo-Garcia, L., Garrido-Mesa, J., et al . (2020). The prebiotic properties of Hibiscus sabdari a extract contribute to the bene cial e ects in diet-induced obesity in mice. Food Res Int, 127 , 108722. doi: 10.1016/j.foodres.2019.108722

Ellulu, M. S., Patimah, I., Khaza'ai, H., Rahmat, A., & Abed, Y. (2017). Obesity and in ammation: the linking mechanism and the complications.Arch Med Sci, 13 (4), 851-863. doi: 10.5114/aoms.2016.58928

Farias, Tdsm, Paixao, R. I. D., Cruz, M. M., de Sa, Rdcdc, Simao, J. J., Antraco, V. J., & Alonso-Vale, M. I. C. (2019). Melatonin Supplementation Attenuates the Pro-In ammatory Adipokines Expression in Visceral Fat from Obese Mice Induced by A High-Fat Diet. Cells, 8 (9). doi: 10.3390/cells8091041

Ferreira-Hermosillo, A., Molina-Ayala, M. A., Molina-Guerrero, D., Garrido-Mendoza, A. P., Ramirez-Renteria, C., Mendoza-Zubieta, V., et al. (2020). E cacy of the treatment with dapagli ozin and met-formin compared to metformin monotherapy for weight loss in patients with class III obesity: a randomized controlled trial. Trials, 21 (1), 186. doi: 10.1186/s13063-020-4121-x

Genario, R., Cipolla-Neto, J., Bueno, A. A., & Santos, H. O. (2021). Melatonin supplementation in the management of obesity and obesity-associated disorders: A review of physiological mechanisms and clinical applications. Pharmacol Res, 163 , 105254. doi: 10.1016/j.phrs.2020.105254

Gonzalez, F. J., & Jiang, C. (2017). A Western diet-induced mouse model reveals a possible mechanism by which metformin decreases obesity.Eur J Clin Pharmacol, 73 (10), 1337-1339. doi: 10.1007/s00228-017-2322-3

Gorwood, P., Benichou, J., Moore, N., Wattez, M., Secouard, M. C., Desobry, X., et al . (2020). Agomelatine in Standard Medical Practice in Depressed Patients: Results of a 1-Year Multicentre Observational Study In France. Clin Drug Investig, 40 (11), 1009-1020. doi: 10.1007/s40261-020-00957-9

Greenblum, S., Turnbaugh, P. J., & Borenstein, E. (2012). Metagenomic systems biology of the human gut microbiome reveals topological shifts associated with obesity and in ammatory bowel disease.Proc Natl Acad Sci U S A, 109 (2), 594-599. doi: 10.1073/pnas.1116053109

Hayashi, T., Fujita, K., Matsushita, M., Hayashi, Y., Uemura, M., & Nonomura, N. (2019). Metformin inhibits prostate cancer growth induced by a high-fat diet in Pten-de cient model mice. Int J Urol, 26 (2), 307-309. doi: 10.1111/iju.13847

Henagan, T. M., Stefanska, B., Fang, Z., Navard, A. M., Ye, J., Lenard, N. R., & Devarshi, P. P. (2015). Sodium butyrate epigenetically modulates high-fat diet-induced skeletal muscle mitochondrial adaptation, obesity and insulin resistance through nucleosome positioning.Br J Pharmacol, 172 (11), 2782-2798. doi: 10.1111/bph.13058

Hickie, I. B., & Rogers, N. L. (2011). Novel melatonin-based therapies: potential advances in the treatment of major depression.Lancet, 378 (9791), 621-631. doi: 10.1016/S0140-6736(11)60095-0

Hussain, M. M., & Pan, X. (2012). Clock regulation of dietary lipid absorption. Curr Opin Clin Nutr Metab Care, 15 (4), 336-341. doi: 10.1097/MCO.0b013e3283548629

Ji, S., Wang, L., & Li, L. (2019). E ect of Metformin on Short-Term High-Fat Diet-Induced Weight Gain and Anxiety-Like Behavior and the Gut Microbiota. Front Endocrinol (Lausanne), 10 , 704. doi: 10.3389/fen-do.2019.00704

Le Chatelier, E., Nielsen, T., Qin, J., Prifti, E., Hildebrand, F., Falony, G., et al . (2013). Richness of human gut microbiome correlates with metabolic markersNature, 500 (7464), 541-546. doi: 10.1038/nature12506

Lee, Y. H., Giraud, J., Davis, R. J., & White, M. F. (2003). c-Jun N-terminal kinase (JNK) mediates feedback inhibition of the insulin signaling cascade.J Biol Chem, 278 (5), 2896-2902. doi: 10.1074/jbc.M208359200

Li, Y., Ma, J., Yao, K., Su, W., Tan, B., Wu, X., et al . (2020). Circadian rhythms and obesity: Timekeeping governs lipid metabolism.J Pineal Res, 69 (3), e12682. doi: 10.1111/jpi.12682

Liu, G., Jiang, Q., Chen, S., Fang, J., Ren, W., Yin, J., et al . (2017). Melatonin alters amino acid metabolism and in ammatory responses in colitis mice.Amino Acids, 49 (12), 2065-2071. doi: 10.1007/s00726-017-2489-z

Loloei, S., Sepidarkish, M., Heydarian, A., Tahvilian, N., Khazdouz, M., Heshmati, J., & Pouraram, H. (2019). The e ect of melatonin supplementation on lipid pro le and anthropometric indices: A systematic review and meta-analysis of clinical trials. Diabetes Metab Syndr, 13(3), 1901-1910. doi: 10.1016/j.dsx.2019.04.043

Louis, P., & Flint, H. J. (2017). Formation of propionate and butyrate by the human colonic microbiota.Environ Microbiol, 19 (1), 29-41. doi: 10.1111/1462-2920.13589

Lu, Q., Li, X., Liu, J., Sun, X., Rousselle, T., Ren, D., et al . (2019). AMPK is associated with the bene cial e ects of antidiabetic agents on cardiovascular diseases.Biosci Rep, 39 (2). doi: 10.1042/BSR20181995

Luther, J., Garber, J. J., Khalili, H., Dave, M., Bale, S. S., Jindal, R., et al. (2015). Hepatic Injury in Nonalcoholic Steatohepatitis Contributes to Altered Intestinal Permeability. Cell Mol Gastroenterol Hepatol, 1 (2), 222-232. doi: 10.1016/j.jcmgh.2015.01.001

Mantele, S., Otway, D. T., Middleton, B., Bretschneider, S., Wright, J., Robertson, M. D., et al . (2012). Daily rhythms of plasma melatonin, but not plasma leptin or leptin mRNA, vary between lean, obese and type 2 diabetic men.PLoS One, 7 (5), e37123. doi: 10.1371/journal.pone.0037123

Milano, W., De Rosa, M., Milano, L., Riccio, A., Sanseverino, B., & Capasso, A. (2013). Successful Treatment with Agomelatine in NES: A Series of Five Cases. Open Neurol J, 7 , 32-37. doi: 10.2174/1874205X20130626001

Muscogiuri, G., Cantone, E., Cassarano, S., Tuccinardi, D., Barrea, L., Savastano, S., et al . (2019). Gut microbiota: a new path to treat obesity. Int J Obes Suppl, 9 (1), 10-19. doi: 10.1038/s41367-019-0011-7

Nogueira, T. C., Lellis-Santos, C., Jesus, D. S., Taneda, M., Rodrigues, S. C., Amaral, F. G., et al.(2011). Absence of melatonin induces night-time hepatic insulin resistance and increased gluconeogenesis due to stimulation of nocturnal unfolded protein response.Endocrinology, 152 (4), 1253-1263. doi: 10.1210/en.2010-1088

O'Neill, L. A., & Hardie, D. G. (2013). Metabolism of in ammation limited by AMPK and pseudo-starvation. Nature, 493 (7432), 346-355. doi: 10.1038/nature11862

Pu, R., Shi, D., Gan, T., Ren, X., Ba, Y., Huo, Y., et al. (2020). E ects of metformin in obesity treatment in di erent populations: a meta-analysis. Ther Adv Endocrinol Metab, 11 , 2042018820926000. doi: 10.1177/2042018820926000

Rebai, R., Jasmin, L., & Boudah, A. (2021). Agomelatine e ects on fat-enriched diet induced neuroin ammation and depression-like behavior in rats. Biomed Pharmacother, 135 , 111246. doi: 10.1016/j.biopha.2021.111246

Reiter, R. J., Tamura, H., Tan, D. X., & Xu, X. Y. (2014). Melatonin and the circadian system: contributions to successful female reproductionFertil Steril, 102 (2), 321-328. doi: 10.1016/j.fertnstert.2014.06.014

Ren, W., Wang, P., Yan, J., Liu, G., Zeng, B., Hussain, T., et al . (2018). Melatonin alleviates weanling stress in mice: Involvement of intestinal microbiota. J Pineal Res, 64 (2). doi: 10.1111/jpi.12448

Rodriguez-Nogales, A., Algieri, F., Garrido-Mesa, J., Vezza, T., Utrilla, M. P., Chueca, N., et al.(2017). Di erential intestinal anti-in ammatory e ects of Lactobacillus fermentum and Lactobacillus salivarius in DSS mouse colitis: impact on microRNAs expression and microbiota composition. Mol Nutr Food Res, 61 (11). doi: 10.1002/mnfr.201700144

Rovella, V., Rodia, G., Di Daniele, F., Cardillo, C., Campia, U., Noce, A., et al. (2021). Association of Gut Hormones and Microbiota with Vascular Dysfunction in Obesity. Nutrients, 13 (2). doi: 10.3390/nu13020613

Ruderman, N. B., Carling, D., Prentki, M., & Cacicedo, J. M. (2013). AMPK, insulin resistance, and the metabolic syndrome. J Clin Invest, 123 (7), 2764-2772. doi: 10.1172/JCI67227

Salminen, A., Hyttinen, J. M., & Kaarniranta, K. (2011). AMP-activated protein kinase inhibits NF-kappaB signaling and in ammation: impact on healthspan and lifespan. J Mol Med (Berl), 89 (7), 667-676. doi: 10.1007/s00109-011-0748-0

Sharma, Mala, McClung, John Arthur, & Abraham, Nader G. (2016). Chapter 4 - Adiponectin: A Mediator of Obesity, Insulin Resistance, Diabetes, and the Metabolic Syndrome. In W. S. Aronow & J. A. McClung (Eds.), Translational Research in Coronary Artery Disease (pp. 33-42). Boston: Academic Press.

Shen, J., Obin, M. S., & Zhao, L. (2013). The gut microbiota, obesity and insulin resistance. Mol Aspects Med, 34 (1), 39-58. doi: 10.1016/j.mam.2012.11.001

Sundara Rajan, S., & Longhi, M. P. (2016). Dendritic cells and adipose tissue. Immunology, 149 (4), 353-361. doi: 10.1111/imm.12653

Targher, G., Byrne, C. D., Lonardo, A., Zoppini, G., & Barbui, C. (2016). Non-alcoholic fatty liver disease and risk of incident cardiovascular disease: A meta-analysis. J Hepatol, 65 (3), 589-600. doi: 10.1016/j.jhep.2016.05.013

Teixeira, T. F., Souza, N. C., Chiarello, P. G., Franceschini, S. C., Bressan, J., Ferreira, C. L., & Peluzio Mdo, C. (2012). Intestinal permeability parameters in obese patients are correlated with metabolic syndrome risk factors. Clin Nutr, 31 (5), 735-740. doi: 10.1016/j.clnu.2012.02.009

WHO. (2019). Obesity and Overweight, World Health Organization.

Wong, J. M., de Souza, R., Kendall, C. W., Emam, A., & Jenkins, D. J. (2006). Colonic health: fermentation and short chain fatty acids. J Clin Gastroenterol, 40 (3), 235-243. doi: 10.1097/00004836-200603000-00015

Woo, S. L., Xu, H., Li, H., Zhao, Y., Hu, X., Zhao, J., et al. (2014). Metformin ameliorates hepatic steatosis and in ammation without altering adipose phenotype in diet-induced obesity. PLoS One, 9 (3), e91111. doi: 10.1371/journal.pone.0091111

Wu, S. J., Huang, W. C., Yu, M. C., Chen, Y. L., Shen, S. C., Yeh, K. W., & Liou, C. J. (2021). Tomatidine ameliorates obesity-induced nonalcoholic fatty liver disease in mice. J Nutr Biochem, 91 , 108602. doi: 10.1016/j.jnutbio.2021.108602

Xu, P., Yin, K., Tang, X., Tian, J., Zhang, Y., Ma, J., et al. (2019). Metformin inhibits the function of granulocytic myeloid-derived suppressor cells in tumor-bearing mice. Biomed Pharmacother, 120 , 109458. doi: 10.1016/j.biopha.2019.109458

Yadav, A., Kataria, M. A., Saini, V., & Yadav, A. (2013). Role of leptin and adiponectin in insulin resistance. Clin Chim Acta, 417 , 80-84. doi: 10.1016/j.cca.2012.12.007

Yin, J., Li, Y., Han, H., Chen, S., Gao, J., Liu, G., et al. (2018). Melatonin reprogramming of gut microbiota improves lipid dysmetabolism in high-fat diet-fed mice. J Pineal Res, 65 (4), e12524. doi: 10.1111/jpi.12524

Zhang, H. M., & Zhang, Y. (2014). Melatonin: a well-documented antioxidant with conditional pro-oxidant actions. J Pineal Res, 57 (2), 131-146. doi: 10.1111/jpi.12162

Zhang, Q., & Hu, N. (2020). E ects of Metformin on the Gut Microbiota in Obesity and Type 2 Diabetes Mellitus. Diabetes Metab Syndr Obes, 13, 5003-5014. doi: 10.2147/DMSO.S286430

Tables

Table 1. qPCR primer sequences.

Gene	Sequence 5'- 3'	Annealing T °C
Adiponectin	FW: GCGAGAGTTTCTGGCAGAGT RV: CCGAGATAGCTGCCAGAGTT	60
Ampk	FW: GACTTCCTTCACAGCCT-CATC RV: CGCGCGACTATCAAAGACATACG	60
Gapdh	FW: CCATCACCATCTTCCAGGAG RV: CCTGCTTCACCACCTTCTTG	60
Glut 4	FW: GAGAATACAGCTAG-GACCAGTG RV: TCTTATTGCAGCAGCGCCTGAG	62
Il-1b	FW: TGATGAGAATGACCTCTTCT RV: CTTCTTCAAAGATGAAGGAAA	60
Il-6	FW: TAGTCCTTCCTACCC-CAATTTCC RV: TTGGTCCTTAGCCACTCCTTCC	60
Jnk-1	FW: GATTTTGGACTGGC-GAGGACT RV: TAGCCCATGCCGAGAATGA	60
Jnk-2	FW: TTGTGCTGCTTTTGAT-ACAGTTCTTGGG RV: CTGGAAAGAGCTCTTCAAATTTGAT	60
Leptin	FW: AGATCCCAGGGAGGAAAATG RV: TGAAGCCCAGGAATGAAGT	60
Leptin R	FW: GCTATTTTGGGAAGATGT RV: TGCCTGGGCCTCTATCTC	60
Muc-2	FW: GCAGTCCTCAGTGGCACCTC RV: CACCGTGGGGCTACTGGAGAG	60
Muc-3	FW: CGTGGTCAACTGCGA-GAATGG RV: CGGCTCTATCTCTACGCTCTCC	60

Occludin	FW: ACGGACCCTGACCACTATGA RV: TCAGCAGCAGCCATGTACTC	56
Ppar- a	FW: TCGAGGAAGGCACTACACCT RV: TCTTCCCAAAGCTCCTTCAA	60
Ppar-g	FW: ACGATCTGCCTGAGGTCTGT RV: CATCGAGGACATCCAAGACA	60
Tlr4	FW: GCCTTTCAGGGAAT-TAAGCTCC RV: AGATCAACCGATGGACGTGTAA	60
Tnf- a	FW: AACTAGTGGTGCCAGCCGAT RV: CTTCACAGAGCAATGACTCC	60
Zo-1	FW: GGGGCCTACACTGATCAAGA RV: TGGAGATGAGGCTTCTGCTT	56

Figure a Legends

Figure 1. Schematic diagram of experiment study design showing mice groups, chronogram, dietary and treatment intervention.

Figure 2. E ects of agomelatine (10, 25 and 50 mg/kg), melatonin (15 mg/kg) and metformin (250 mg/kg) administration on (A) body weight evolution; (B) energy intake and energy e ciency, and; (C) epididymal and abdominal fat in high fat diet (HFD)-fed mice. Data are expressed as means ± SEM (n=8). Groups with di erent letters statistically di er ($p < 0.05$).

Figure 3. Result of the administration of agomelatine (10, 25 and 50 mg/kg), melatonin (15 mg/kg) and metformin (250 mg/kg) on (A) glucose tolerance test and area under the curve (AUC); (B) basal glucose, insulin levels, and HOMA-IR index; and (C) Total, LDL- and HDL- Cholesterol plasma levels in high fat diet (HFD) group. Data are expressed as means ± SEM (n=8). Groups with di erent letters statistically di er ($p < 0.05$).

Figure 4. Impact of agomelatine (10, 25 and 50 mg/kg), melatonin (15 mg/kg) and metformin (250 mg/kg) administration on in ammatory status. (A) Fat and liver gene expression of Tnf-a , Il-1b , Il-6 and Mcp-1 ; (B) Liver gene expression of Jnk-1 ; (C) fat gene expression of Leptin , Leptin receptor , and Adiponectin and liver expression of Leptin receptor; (D) fat and liver gene expression of Glut-4 and Ampk in high fat diet (HFD)-fed mice. Data are expressed as means ± SEM (n=8). Groups with di erent letters statistically di er ($p < 0.05$).

Figure 5. E ects of agomelatine (10, 25 and 50 mg/kg), melatonin (15 mg/kg) and metformin (250 mg/kg) administration on hepatic Total, $Ly6C^+ CD11b^+$ and $CD45^+ CD11b^{int}$ immune-cell populations, and total and $CD45^+ CD11b^{int}$ immune-cell populations in adipose tissue in high fat diet (HFD)-fed mice. Data are expressed as means ± SEM (n=8). Groups with di erent letters statistically di er ($p < 0.05$).

Figure 6. In uence of agomelatine (10, 25 and 50 mg/kg), melatonin (15 mg/kg) and metformin (250 mg/kg) administration on (A) colonic gene expression of Muc-2 , Muc-3 , Occludin , T -3 and Zo-1 , and;

(B) hepatic gene expression of Tlr-4 in high fat diet (HFD)-fed mice. Data are expressed as means ± SEM (n=8). Groups with di erent letters statistically di er ($p < 0.05$).

Figure 7. Impact of the administration of agomelatine (50 mg/kg), melatonin (15 mg/kg) and metformin (250 mg/kg) on (A) microbiota diversity (Chao1, Shannon index and Observed OTUs); (B) beta-diversity by principal coordinate analysis score plot, and; (C) bacterial phyla and F/B ratio in high fat diet (HFD)-fed mice. Data are expressed as means ± SEM (n=8). Groups with di erent letters statistically di er ($p < 0.05$).

Figure 8. E ect of agomelatine (50 mg/kg), melatonin (15 mg/kg) and metformin (250 mg/kg) administration on microbiota diversity at the order level in high fat diet (HFD)-fed mice. Data are expressed as means ± SEM (n=8). Groups with di erent letters statistically di er ($p < 0.05$).

Figure 9. (A) Metagenomic functional features predicted by PICRUSt (Phylogenetic Investigation of Communities by Reconstruction of Unobserved States) that were di erentially abundant and drove di erences in control, untreated and agomelatine, melatonin or metformin treated HFD-fed mice. E ect of the administration of agomelatine (50 mg/kg), melatonin (15 mg/kg) and metformin (250 mg/kg) on the (B) Relative abundance of short fatty acid (SCFA)-producing bacteria, and on the (C) Acetate:Propionate ratio in high fat diet (HFD)-fed mice. Data are expressed as means ± SEM (n=8). Groups with di erent letters statistically di er ($p < 0.05$).

Figure 10. E ect of agomelatine (10, 25 and 50 mg/kg), melatonin (15 mg/kg) and metformin (250 mg/kg) administration on (A) aortic endothelial function, and; (B) aortic NADPH activity in high fat diet (HFD)-fed mice. Data are expressed as means ± SEM (n=8). Groups with di erent letters statistically di er ($p < 0.05$).

Figure 2

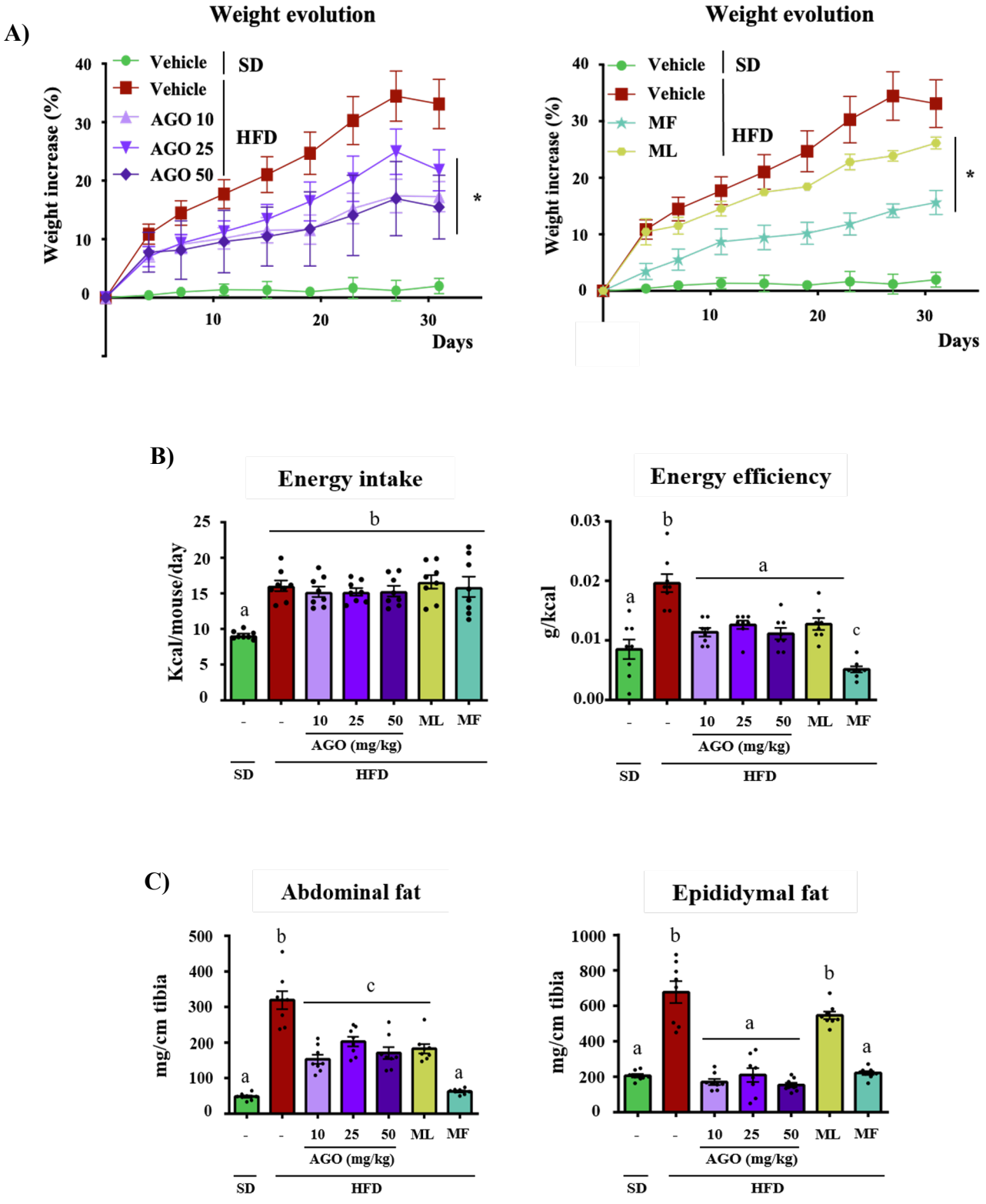
A)
Weight evolution
Weight increase (%)
Vehicle
Vehicle
AGO 10
AGO 25
AGO 50
SD
HFD
*
Days
Weight evolution
Vehicle
Vehicle
MF
ML
SD
HFD
*
Days
B)
Energy intake
Kcal/mouse/day
AGO (mg/kg)
SD
HFD
Energy efficiency
g/kcal
AGO (mg/kg)
SD
HFD
C)
Abdominal fat
mg/cm tibia
AGO (mg/kg)
SD
HFD
Epididymal fat
mg/cm tibia
AGO (mg/kg)
SD
HFD

Figure 3

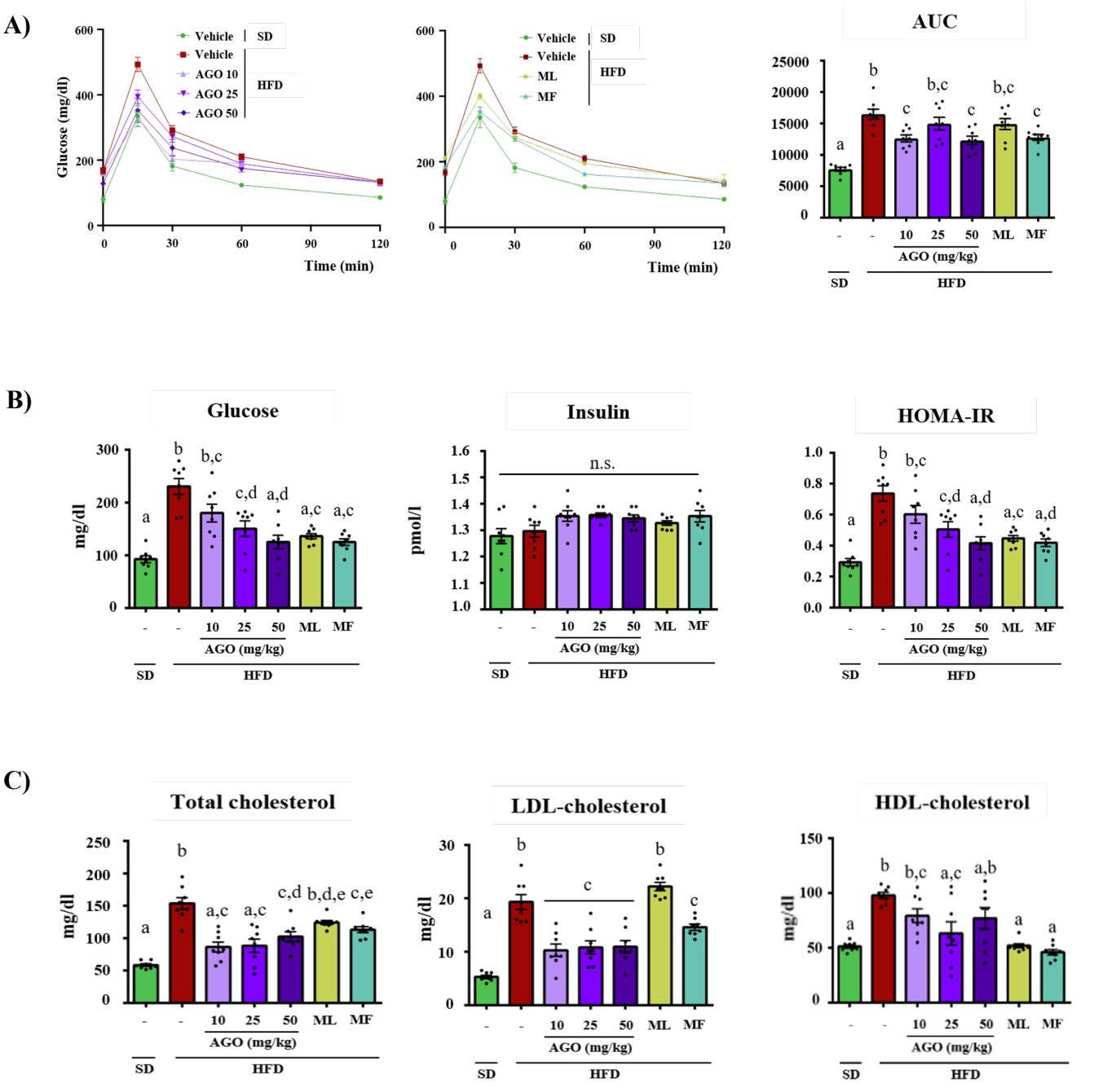
A)
Vehicle
Vehicle
AGO 10
AGO 25
AGO 50
SD
HFD
Glucose (mg/dl)
Time (min)
Vehicle
Vehicle
ML
MF
AUC
AGO (mg/kg)
B)
Glucose
Insulin
HOMA-IR
mg/dl
pmol/l
n.s.
C)
Total cholesterol
LDL-cholesterol
HDL-cholesterol

Figure 4

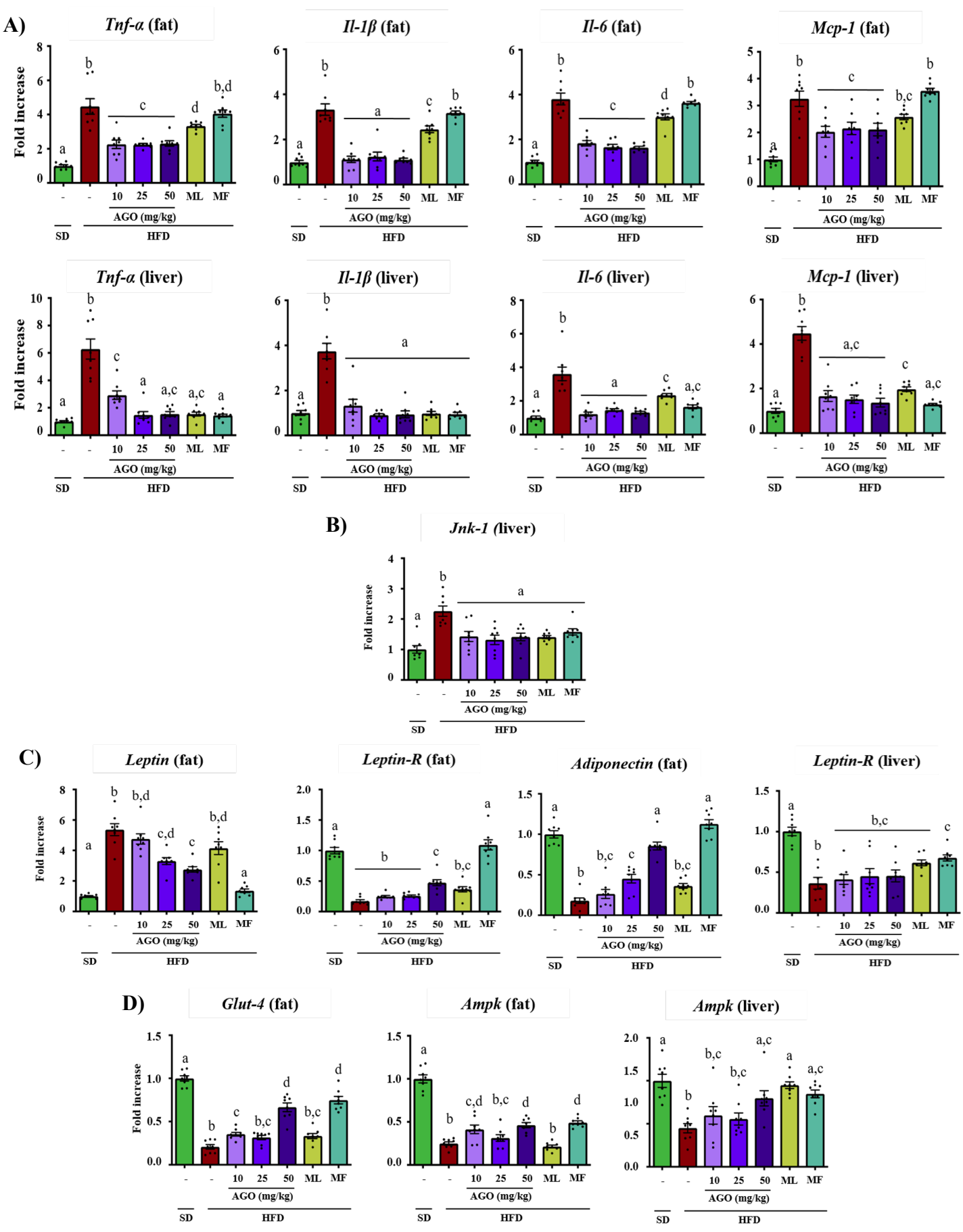
A)
Tnf-α (fat)
Il-1β (fat)
Il-6 (fat)
Mcp-1 (fat)
Tnf-α (liver)
Il-1β (liver)
Il-6 (liver)
Mcp-1 (liver)
Fold increase
- - 10 25 50 ML MF
AGO (mg/kg)
SD
HFD
B)
Jnk-1 (liver)
C)
Leptin (fat)
Leptin-R (fat)
Adiponectin (fat)
Leptin-R (liver)
D)
Glut-4 (fat)
Ampk (fat)
Ampk (liver)

Figure 5

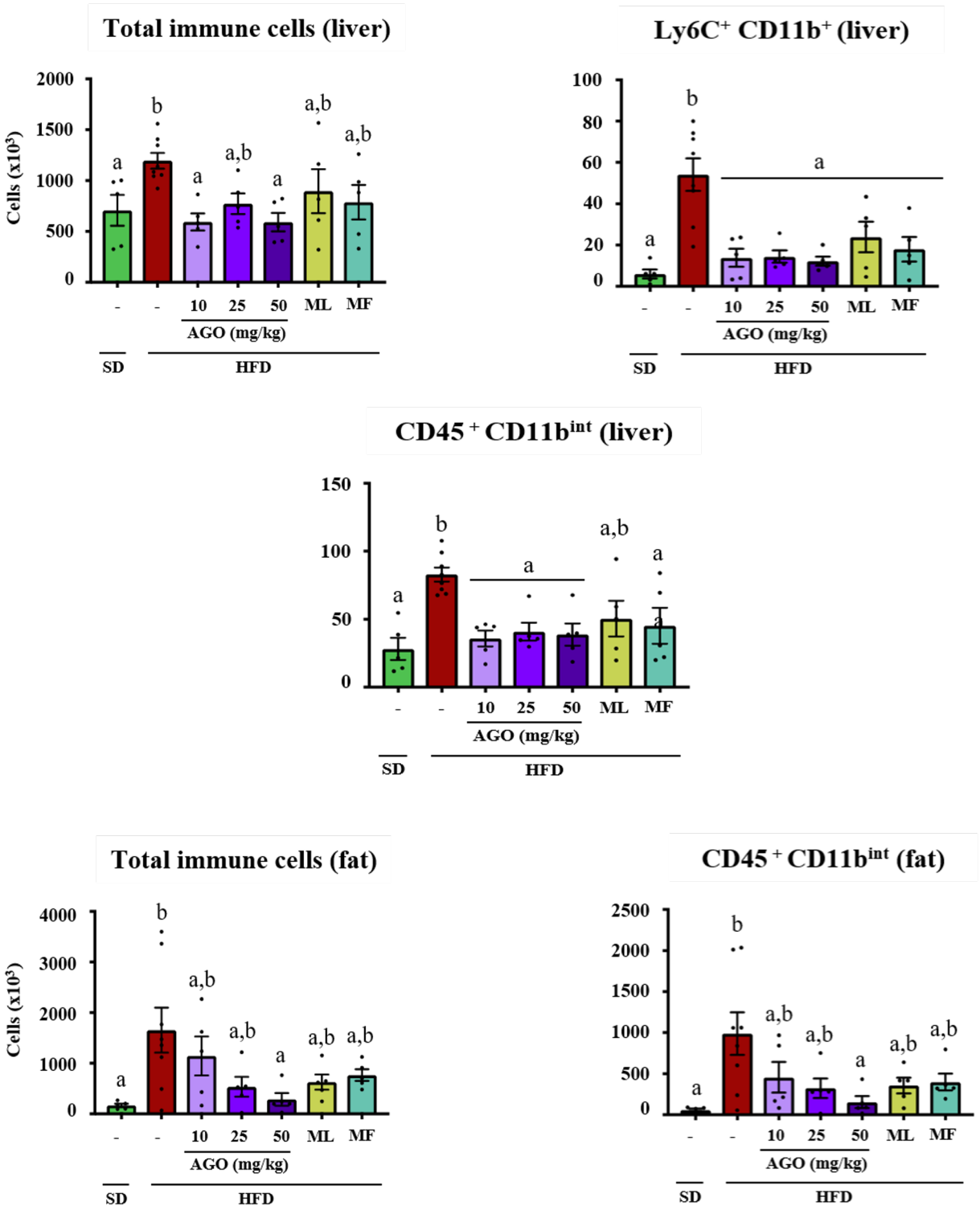
Total immune cells (liver)
Cells (x10³)
2000
1500
1000
500
0
a
b
a
a,b
a
a,b
a,b
- - 10 25 50 ML MF
AGO (mg/kg)
SD
HFD
Ly6C⁺ CD11b⁺ (liver)
100
80
60
40
20
0
a
b
a
- - 10 25 50 ML MF
AGO (mg/kg)
SD
HFD
CD45⁺ CD11b^int (liver)
150
100
50
0
a
b
a
a,b
a
- - 10 25 50 ML MF
AGO (mg/kg)
SD
HFD
Total immune cells (fat)
Cells (x10³)
4000
3000
2000
1000
0
a
b
a,b
a,b
a
a,b
a,b
- - 10 25 50 ML MF
AGO (mg/kg)
SD
HFD
CD45⁺ CD11b^int (fat)
2500
2000
1500
1000
500
0
a
b
a,b
a,b
a
a,b
a,b
- - 10 25 50 ML MF
AGO (mg/kg)
SD
HFD

Figure 6

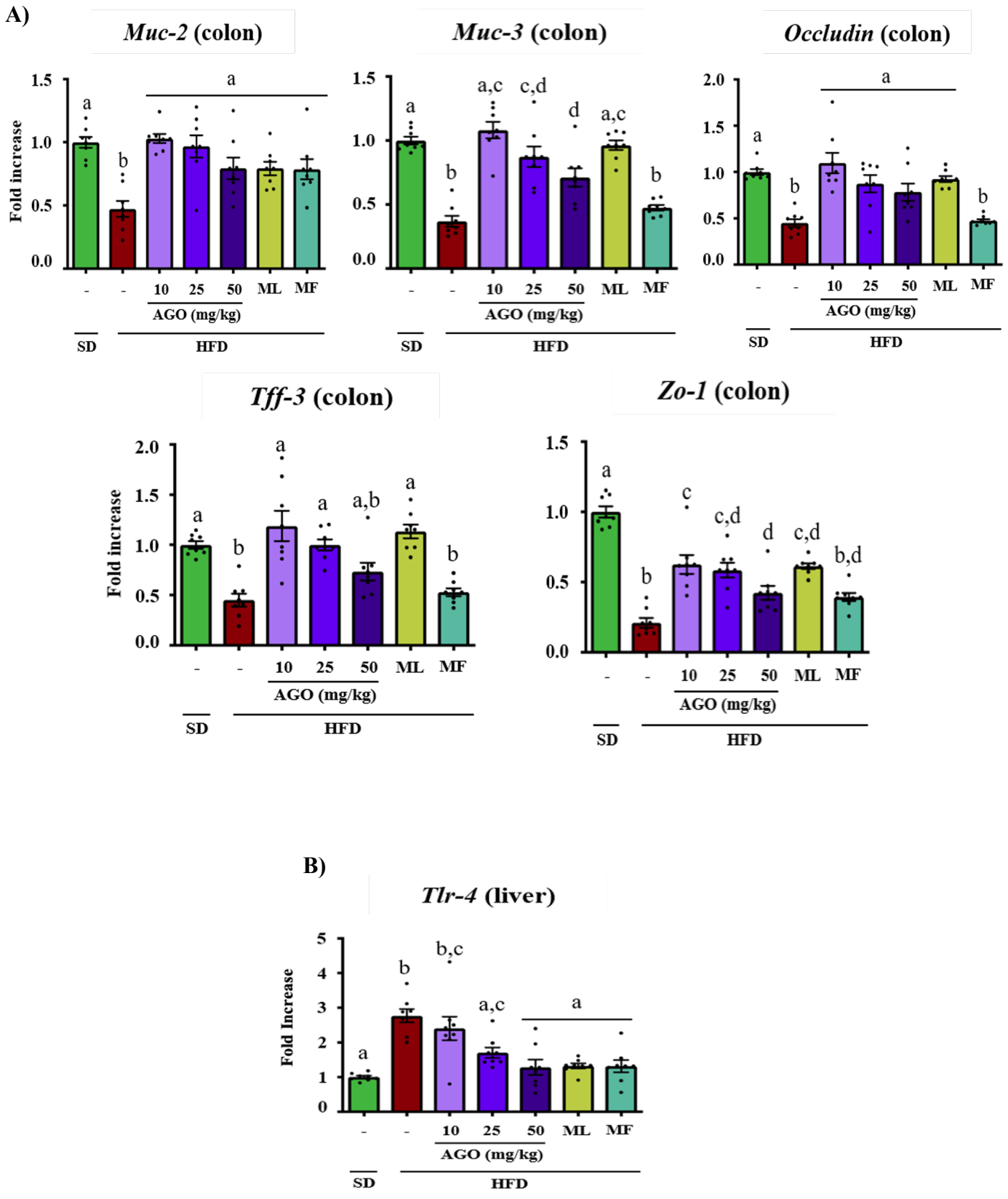
A)
Muc-2 (colon)
Muc-3 (colon)
Occludin (colon)
Tff-3 (colon)
Zo-1 (colon)
Fold increase
AGO (mg/kg)
SD
HFD
B)
Tlr-4 (liver)
Fold Increase

Figure 7

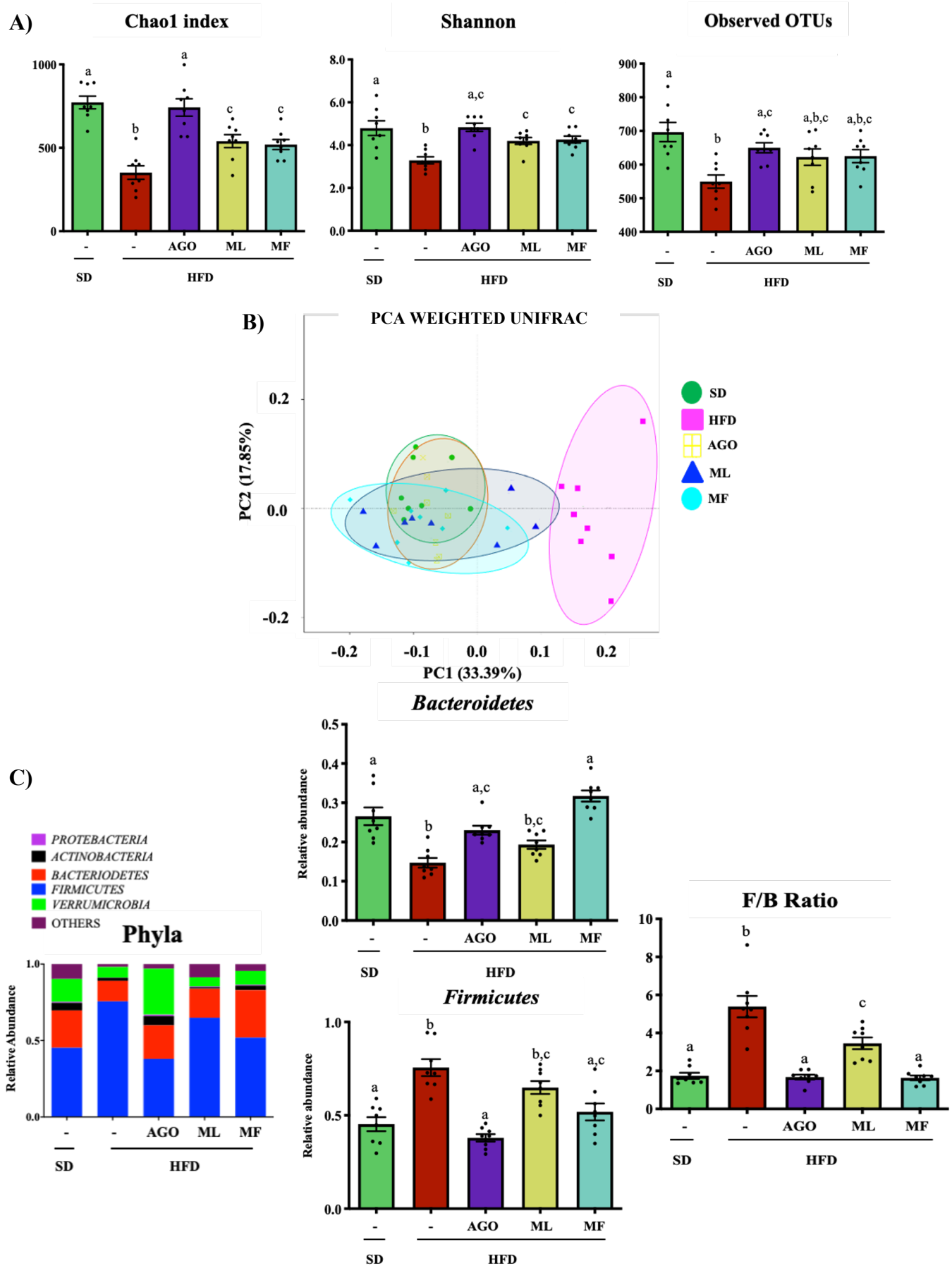
A)
Chao1 index
Shannon
Observed OTUs
SD
HFD
AGO
ML
MF
B)
PCA WEIGHTED UNIFRAC
PC2 (17.85%)
PC1 (33.39%)
C)
PROTEBACTERIA
ACTINOBACTERIA
BACTERIODETES
FIRMICUTES
VERRUMICROBIA
OTHERS
Phyla
Relative Abundance
Bacteroidetes
Firmicutes
Relative abundance
F/B Ratio

Figure 8

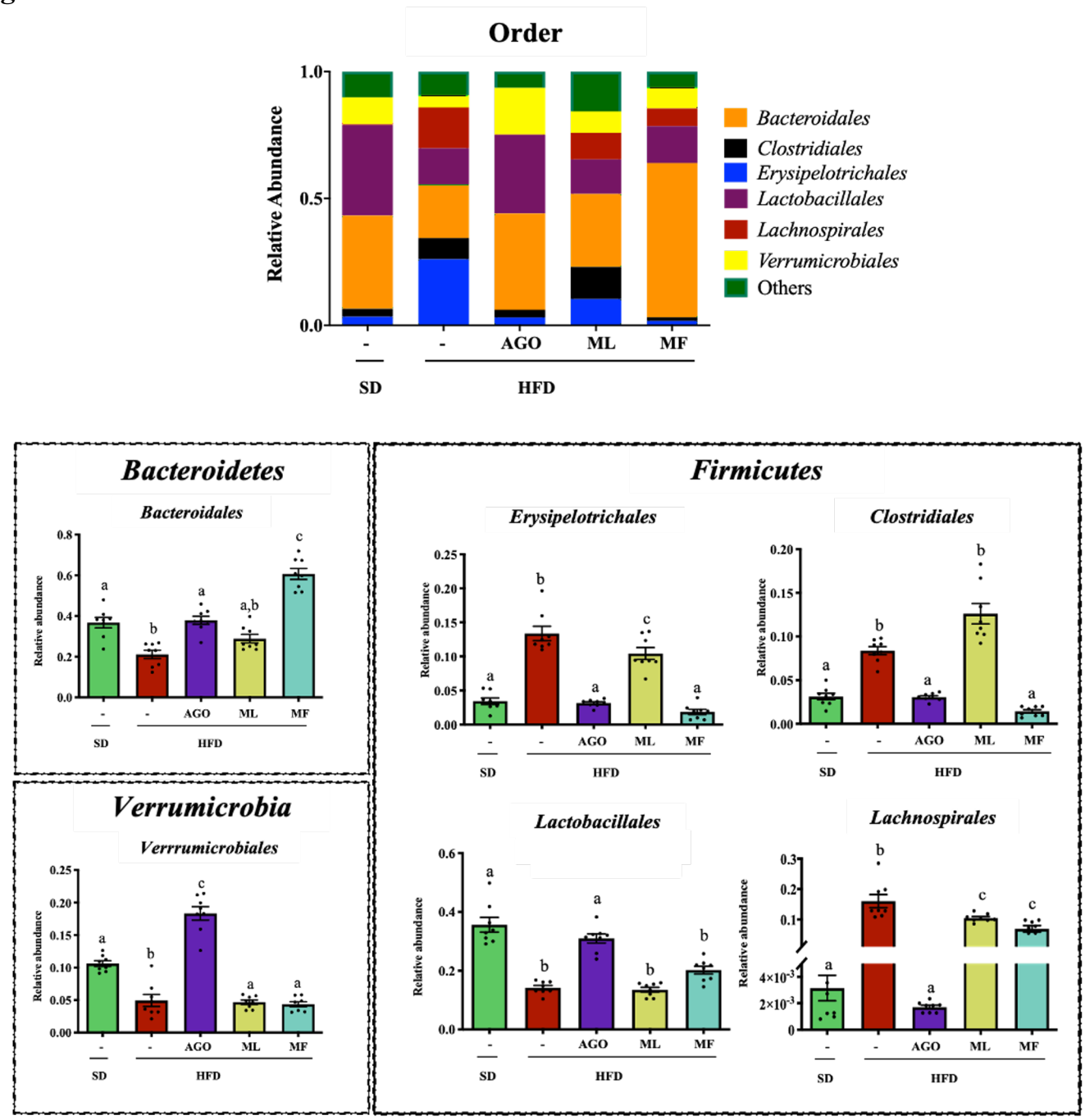
Order
Relative Abundance
1.0
0.5
0.0
Bacteroidales
Clostridiales
Erysipelotrichales
Lactobacillales
Lachnospirales
Verrumicrobiales
Others
-
-
AGO
ML
MF
SD
HFD
Bacteroidetes
Bacteroidales
Firmicutes
Erysipelotrichales
Clostridiales
Verrumicrobia
Verrrumicrobiales
Lactobacillales
Lachnospirales
Relative abundance

Figure 9

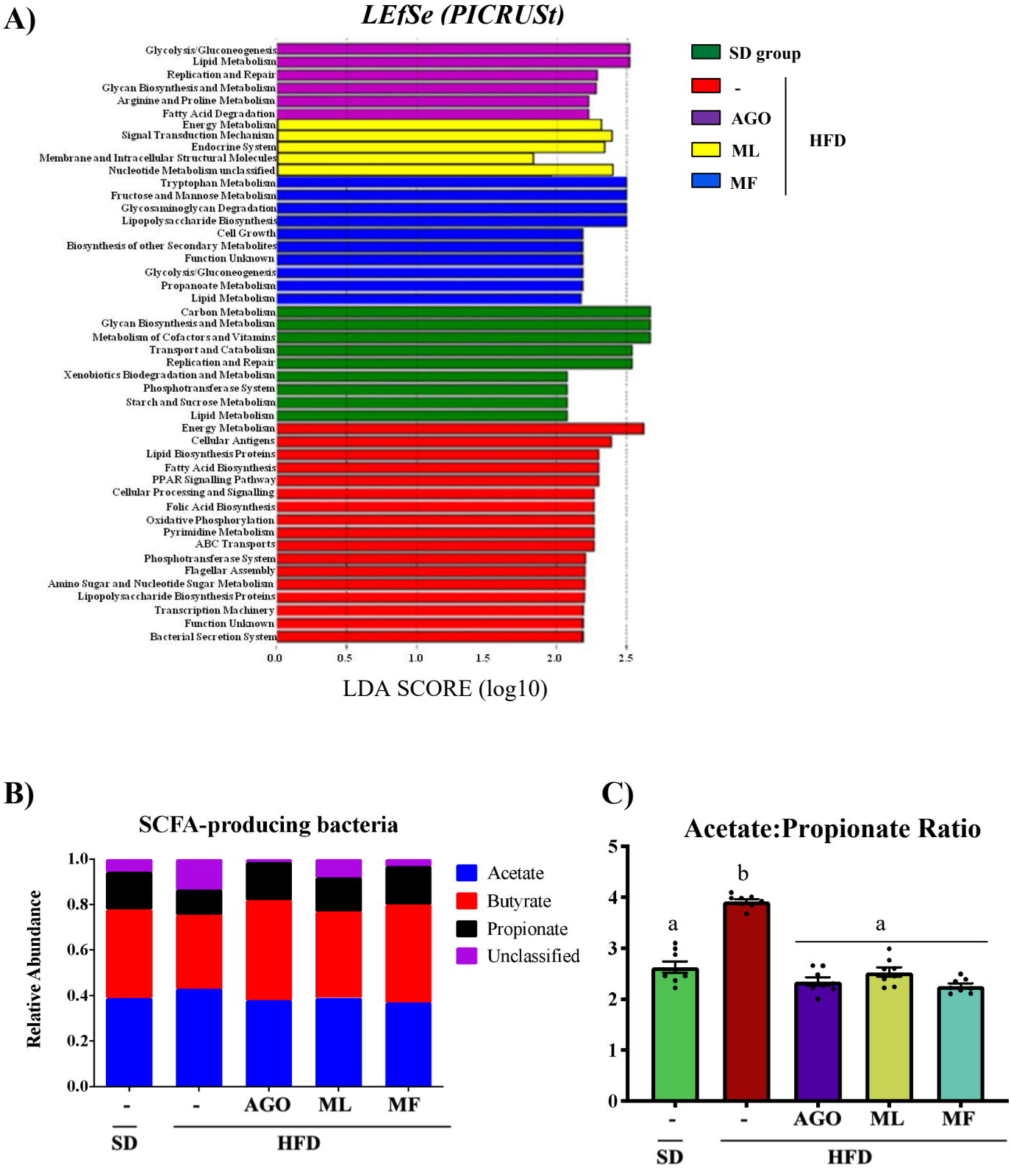
A)
LEfSe (PICRUSt)
Glycolysis/Gluconeogenesis
Lipid Metabolism
Replication and Repair
Glycan Biosynthesis and Metabolism
Arginine and Proline Metabolism
Fatty Acid Degradation
Energy Metabolism
Signal Transduction Mechanism
Endocrine System
Membrane and Intracellular Structural Molecules
Nucleotide Metabolism unclassified
Tryptophan Metabolism
Fructose and Mannose Metabolism
Glycosaminoglycan Degradation
Lipopolysaccharide Biosynthesis
Cell Growth
Biosynthesis of other Secondary Metabolites
Function Unknown
Glycolysis/Gluconeogenesis
Propanoate Metabolism
Lipid Metabolism
Carbon Metabolism
Glycan Biosynthesis and Metabolism
Metabolism of Cofactors and Vitamins
Transport and Catabolism
Replication and Repair
Xenobiotics Biodegradation and Metabolism
Phosphotransferase System
Starch and Sucrose Metabolism
Lipid Metabolism
Energy Metabolism
Cellular Antigens
Lipid Biosynthesis Proteins
Fatty Acid Biosynthesis
PPAR Signalling Pathway
Cellular Processing and Signalling
Folic Acid Biosynthesis
Oxidative Phosphorylation
Pyrimidine Metabolism
ABC Transports
Phosphotransferase System
Flagellar Assembly
Amino Sugar and Nucleotide Sugar Metabolism
Lipopolysaccharide Biosynthesis Proteins
Transcription Machinery
Function Unknown
Bacterial Secretion System
0.0
0.5
1.0
1.5
2.0
2.5
LDA SCORE (log10)
SD group
-
AGO
ML
MF
HFD
B)
SCFA-producing bacteria
Relative Abundance
1.0
0.8
0.6
0.4
0.2
0.0
Acetate
Butyrate
Propionate
Unclassified
-
-
AGO
ML
MF
SD
HFD
C)
Acetate:Propionate Ratio
5
4
3
2
1
0
a
b
a
-
-
AGO
ML
MF
SD
HFD

Figure 10

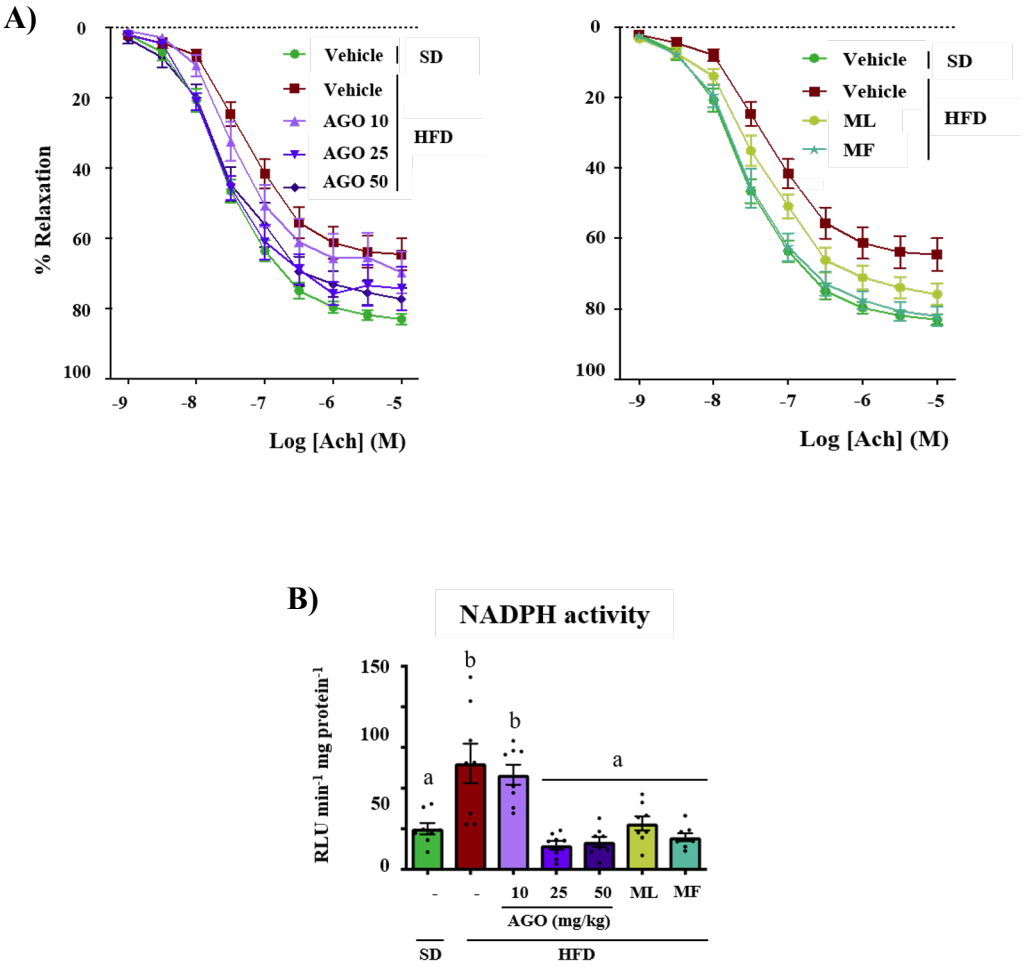
A)
% Relaxation
Log [Ach] (M)
Vehicle
Vehicle
AGO 10
AGO 25
AGO 50
SD
HFD
Vehicle
Vehicle
ML
MF
SD
HFD
B)
NADPH activity
RLU min-1 mg protein-1
AGO (mg/kg)
SD
HFD
ML
MF